UNIVERSITYOF BIRMINGHAM

Research at Birmingham

Alkanes and Aliphatic Carbonyl Compounds in Wintertime PM2.5 in Beijing, China

Lyu, Ruihe; Shi, Zongbo; Alam, Mohammed; Wu, Xuefang; Liu, Di; VU, Van Tuan; Stark, Christopher; Xu, Ruixin; Fu, Pingqing; Feng, Yinchang; Harrison, Roy

Link to publication on Research at Birmingham portal

Alkanes and aliphatic carbonyl compounds in wintertime PM$_{2.5}$ in Beijing, China

Ruihe Lyu[a,b], Zongbo Shi[b,c], Mohammed Salim Alam[b], Xuefang Wu[b,d], Di Liu[b], Tuan V. Vu[b], Christopher Stark[b], Ruixin Xu[b], Pingqing Fu[c,e], Yinchang Feng[a,**], Roy M. Harrison[b,*,1]

[a] State Environmental Protection Key Laboratory of Urban Ambient Air Particulate Matter Pollution Prevention and Control, College of Environmental Science and Engineering, Nankai University, Tianjin, 300350, China
[b] Division of Environmental Health and Risk Management, School of Geography, Earth and Environmental Sciences, University of Birmingham, Edgbaston, Birmingham, B15 2TT, UK
[c] Institute of Surface-Earth System Science, Tianjin University, Tianjin, 300350, China
[d] School of Geology and Mineral Resources, China University of Geosciences Xueyuan Road 29, 100083, Beijing, China
[e] State Key Laboratory of Atmospheric Boundary Layer Physics and Atmospheric Chemistry, Institute of Atmospheric Physics, Chinese Academy of Sciences, Beijing, 100029, China

ABSTRACT

Organic aerosol is one of the dominant components of PM$_{2.5}$ in megacities. In order to understand the sources and formation processes of aliphatic carbonyl compounds, the concentrations of saturated and unsaturated aliphatic hydrocarbons and carbonyl compounds were determined in the PM$_{2.5}$ from an urban area of Beijing sampled in November–December 2016 and analysed using two dimensional gas chromatography coupled to time-of-flight mass spectrometry (GC x GC-TOFMS). The data were separated into non-haze and haze days (PM$_{2.5} \geq 75 \, \mu g \, m^{-3}$). n-Alkanes (C$_{10}$-C$_{36}$) and n-alkenes (C$_{12}$-C$_{26}$) were abundant in the samples during the sampling campaign regardless of non-haze and haze conditions, and the middle chain length n–alkanes (C$_{25}$–C$_{34}$) were the most abundant. Aliphatic carbonyls, specifically n-alkanals (C$_8$-C$_{29}$), n-alkan-2-ones (C$_8$-C$_{31}$) and n-alkan-3-ones (C$_8$-C$_{30}$) were also detected in the PM$_{2.5}$ at concentrations much lower than n-alkanes. The n-alkanals were the most abundant compounds amongst the aliphatic carbonyls, accounting for 65.4% on average of the total mass of aliphatic carbonyls. For the non-haze days, it seems likely that the OH oxidation of n-alkanes was a source of carbonyl compounds, whereas vehicle exhaust makes a significant contribution to the n-alkanes and n-alkanals, but makes a much smaller contribution to the n-alkan-2-ones and n-alkan-3-ones. It appears that primary sources are likely to be a major contributor to concentrations of the high molecular weight carbonyl compounds during the haze episodes, probably deriving from coal combustion. In addition, furanones (γ-lactones) and phytone (6, 10, 14-trimethylpentadecan-2-one) were also detected in our samples and are oxidation products of hydrocarbons and a marker of biogenic input, respectively. Cooking emissions also appear to be a likely contributor to the furanones. This study provides new information on the profiles of PM$_{2.5}$-associated aliphatic hydrocarbons and carbonyl compounds, and gives insights into their sources. Differences in the concentrations and ratios of carbonyl compounds between Beijing and London are discussed.

1. Introduction

Ambient aerosols have received much attention due to their potential impact on air quality, climate change, and human health (Seinfeld and Pandis, 2016). Organic compounds account for a large fraction of atmospheric particulate matter (PM), especially the particles with an aerodynamic diameter less than 2.5 μm (PM$_{2.5}$). About 40–60% of the fine aerosol mass is composed of organic materials (Huang et al., 2014) which are generated from anthropogenic and biogenic sources, and many organic constituents in PM$_{2.5}$ are recognized as mutagenic or carcinogenic compounds. Fossil fuel combustion including vehicular exhaust, biomass burning and industrial activities are considered as the

---

major primary emission sources for organic compounds (Zhu et al., 2016), while secondary organic aerosol (SOA) is formed by the oxidation of gas-phase precursors, originating either locally or through long-range transport in the atmosphere.

Measurements of specific compounds can provide information on the sources of organic substances. The n-alkanes have been extensively studied and are one of the most important precursors of SOA (Presto et al., 2010). The n-alkenes have larger rate coefficients for reaction with atmospheric oxidants and are considered as an important class of volatile organic compound (VOC) precursors in ozone formation. Both n-alkanes and n-alkenes are directly emitted from primary emission sources (e.g., fossil fuel combustion, petroleum residues, biomass burning, cooking process, higher plants wax, bacteria, pollen, and insects) (Rogge et al., 1993; Simoneit, 1989), and are abundant compounds in atmospheric particulate matter (Lyu et al., 2017; Hong et al., 2017). The higher molecular weight carbonyl compounds, including n-alkanones, and furanones, have been identified in atmospheric particulate matter in several cities (Gogou et al., 1996; Andreou and Rapsomanikis, 2009). Such polar organic compounds are emitted directly into the atmosphere as PM by a multiplicity of sources including coal combustion (Oros and Simoneit, 2000), vehicular emissions (Schauer et al., 2002), cooking processes (Schauer et al., 1999a) and biomass burning (Rogge et al., 1998), as well as being products of secondary organic aerosol (SOA) formation via photochemical reactions of hydrocarbons initiated by ozone and hydroxyl or nitrate radical.

Beijing is the capital of China and is one of the major cities of the world. With the growing urbanization, increasing vehicle numbers, rapid economic development, and large energy consumption, Beijing has been suffering from serious air pollution over the past two decades. Both anthropogenic and biogenic emission sources contribute to the atmospheric fine particles (PM$_{2.5}$), which are the most serious environmental issue in Beijing nowadays (Huang et al., 2014). The annual average concentration of PM$_{2.5}$ in Beijing was 69.7–122.4 $\mu g\,m^{-3}$ during the past decade (Lang et al., 2017), 2.0–3.5 times the national standard (35 $\mu g\,m^{-3}$). The average PM$_{2.5}$ concentration during the winter period from November 2014 to March 2015 was 96 $\mu g\,m^{-3}$ in Beijing, which was 9.6 times the World Health Organization (WHO) annual mean guideline of 10 $\mu g/m^3$. As a result, PM$_{2.5}$ has received a great deal of attention in recent studies (Yao et al., 2016; Ren et al., 2016; Li et al., 2013; Feng et al., 2006). Due to the frequent haze events in Beijing, the Beijing government has applied a series of control measures in recent years, especially after the 2008 Olympics, which may greatly influence primary and secondary particle sources and the nature of haze episodes may be changing. Organic matter comprises a substantial proportion of the atmospheric particulate matter in Beijing and other Chinese cities (Wu et al., 2018).

n-Alkanes are common species in primary emissions and have been widely used to identify the different sources of particles. In general, higher molecular weight n-alkanes ($> C_{25}$) with a significant odd carbon number predominance are mainly originated from the leaf wax of higher plants (Simoneit, 1989), which can enter the atmosphere through direct wind abrasion, leaves rubbing together or biomass burning and forest fires (Chrysikou and Samara, 2009), while n-alkanes derived from fossil fuels show no or weak carbon number preference (Bi et al., 2003). As the most abundant organic compounds in the ambient aerosol, the concentrations of n-alkanes could be up to few micrograms per cubic-metre. Table 1 reviews the previous studies of n-alkanes in China. Ren and coworkers reported that the concentrations of n-alkanes (C_{19}–C_{36}) ranged from 40.1 to 1720 ng m^{-3} (average 367 ng m^{-3}) (Ren et al., 2016), and these concentrations are comparable to those (573 ng m^{-3}) reported in wintertime samples in fourteen Chinese megacities (Wang et al., 2006).

Long chain carbonyl compounds, including n-alkanals, n-alkan-2-ones and n-alkan-3-ones have been reported in a few published articles (Andreou and Rapsomanikis, 2009; Oliveira et al., 2007). The n-alkanals have been found to originate mainly from primary anthropogenic

sources with n-alkanes. On the other hand, the alkanones probably originate from atmospheric photochemical reactions of n-alkanes, and have been identified amongst the reaction products of n-alkanes during chamber and flow tube studies (Zhang et al., 2015; Ruehl et al., 2013).

The objective of this study was to investigate the n-alkanes, n-alkenes and aliphatic carbonyl components in PM$_{2.5}$ samples collected in Beijing during wintertime, 2016, and to compare with the much less polluted atmosphere of London, where pollution controls have been developed over the past 60 years. Both cities have very heavy road traffic, but the light duty (passenger car) vehicle fleet in London is around 50% diesel and dominates the primary particle emissions, while Beijing has a fleet of mainly gasoline-powered cars. Here, we report the concentration and molecular distributions of seven organic compound classes (more than 100 organic species) in the fine aerosol. Based on the diagnostic criteria, we report their possible sources, formation processes, and reveal and assess their pollution characteristics in non-haze and haze periods. Finally, the concentrations and distributions of carbonyl compounds were compared with our previous studies in order to assess and understand the differences between the two metropolitan regions (Beijing and London).

2. Materials and methods

2.1. Sampling method and site characteristics

PM$_{2.5}$ samples were collected at the Institute of Atmospheric Physics (IAP), Chinese Academy of Sciences in Beijing, China. The sampling site (89°58′28″ N, 11°62′16″ E) was located between the North 3rd Ring Road and North 4th Ring Road (Fig. 1). The site is 8 m above ground, approximately 1 km from the 3rd Ring Road, 200 m west of the G6 Highway (which runs north-south) and 50 m south of Beitucheng West Road (which runs east-west). The annual average vehicular speeds in the morning and evening traffic peak were 27.4 and 24.3 km h^{-1}, respectively. No industrial sources were located in the vicinity of the sampling site. The experimental campaign was launched from November 9 to December 11, 2016. The samples were collected onto pre-baked (450 °C for 6 hours) quartz fibre filters (Pallflex) by a high-volume sampler (Tisch, USA) at a flow rate of 1.0 m^3 min^{-1} during the sampling period. The collecting time was 24 h per sample and three blank samples were collected during this period. After sampling, each filter was packed separately and stored in a freezer at −20 °C until the analysis. The London samples were collected between 24 January and 19 February 2017 at Regent's University which is close to the southern boundary of Regent's Park, and about 350 m from the heavily trafficked Marylebone Road. The sampler is located on a rooftop, about 16 m above ground.

2.2. Analytical instrumentation

The particle samples were analyzed using a 2D gas chromatograph (GC, 7890A, Agilent Technologies, Wilmington, DE, USA) equipped with a Zoex ZX2 cryogenic modulator (Houston, TX, USA). The first dimension was equipped with a SGE DBX5, non-polar capillary column (30.0 m, 0.25 mm ID, 0.25 mm–5.00% phenyl polysilphenylene-siloxane), and the second-dimension column equipped with a SGE DBX50 (4.00 m, 0.10 mm ID, 0.10 mm–50.0% phenyl polysilphenylene-siloxane). The GC x GC was interfaced with a Bench-ToF-Select, time-of-flight mass spectrometer (ToF-MS, Markes International, Llantrisant, UK). The acquisition speed was 50.0 Hz with a mass resolution of > 1200 fwhm at 70.0 eV and the mass range was 35.0–600 m/z. All data produced were processed using GC Image v5.4 (Zoex Corporation, Houston, US).

2.3. Analysis of samples

Standards used in these experiments included 19 alkanes, C_8 to C_{26}

Table 1
Comparison of concentrations (ng m^{-3}) and diagnostic parameters for n-alkanes with other cities around China (the sequence of study sites is from the north to south China).

Location	Sampling period	Range	Sampling type	Σ n-alkanes	CPI	Cmax	WNA %	Reference
IAP, Urban, Beijing	2016.11–2016.12	C_{10}-C_{35}	PM$_{2.5}$	450.1 ± 315.6	1.27	C_{25}	14.8	Present study
Beijing	2012.01	C_{19}-C_{36}	TSP	367	1.5	C_{23}, C_{25}	17	Ren et al. (2016)
IAP, Urban, Beijing	2006 Spring	C_{19}-C_{25}	PM$_{2.5}$	205 ± 128	1.20 ± 0.15	C_{22}	13 ± 7.5	Li et al. (2013)
	2006 Summer			179 ± 112	1.18 ± 0.13		22 ± 29	
	2006 Autumn			323 ± 130	1.44 ± 0.37		48 ± 20	
	2006 Winter			420 ± 110	1.20 ± 0.07		41 ± 24	
Beijing	2004	C_{20}-C_{35}	PM$_{2.5}$	163 ± 193		C_{29}		Feng et al. (2006)
Tianjin	2007.04–2008.01	C_{12}-C_{35}	PM$_{2.5}$	413.6	1.19	C_{27}, C_{31}	19.4	Li et al. (2010)
Shanghai	2012 Winter	C_8-C_{40}	PM$_{10}$	262.7	1.2	C_{25}	19	Lyu et al. (2017)
	2013 Spring			208	1.5	C_{25}	23	
	2013 Summer			180.4	1.4	C_{29}	30	
	2013 Autumn			283.9	1.6	C_{29}	28	
Shanghai	2014.11–2015.8	C_{16}-C_{40}	PM$_{2.5}$	93.7	1.58	C_{29}, C_{27}	47.5	Hong et al. (2017)
Shanghai	2009.09	C_{17}-C_{40}	PM$_{2.5}$	32.2	1.33	C_{29}	17	Cao et al. (2013)
Shanghai	2003–2003	C_{17}-C_{36}	PM$_{2.5}$	32–341.9		C_{29}, C_{31}		Feng et al. (2006)
Nanjing	2014.11–2015.08	C_{16}-C_{40}	PM$_{2.5}$	83.5	1.62	C_{29}	50.1	Hong et al. (2017)
Nanjing	2004 summer	C_{18}-C_{36}	PM$_{2.5}$	68.2	2.7	C_{29}		Wang et al. (2005)
	2005 winter			22.5	1.3	C_{22}, C_{23}		Hong et al. (2017)
Ningbo	2014.11–2015.08	C_{16}-C_{40}	PM$_{2.5}$	184.3	1.34	C_{29}, C_{27}	34.5	Han et al. (2018)
Jiujiang	2016.09–2016.12	C_{11}-C_{40}	PM$_{2.5}$	105.3 ± 55.1 (16.3 ± 305.0)	1.00–1.79	C_{31}	17	Wang et al. (2016) Wang et al. (2005)
Guangzhou	2012 summer	C_{22}-C_{38}	PM$_{2.5}$	26.2	1.1	C_{29}, C_{31}	12	Hong et al. (2017)
	2012 winter			102.7	1.3	C_{29}, C_{31}	17.3	
Guangzhou	2010.11	C_{19}-C_{40}	PM$_{2.5}$	48.1 ± 20.8	1.2-1.7	C_{29}	19.5	Xu et al. (2013)

(Sigma-Aldrich, UK, purity > 99.2%); 12 n-aldehydes, C_8 to C_{13} (Sigma-Aldrich, UK, purity ≥95.0%), C_{14} to C_{18} (Tokyo Chemical Industry UK Ltd, purity > 95.0%); and 10 2-ketones, C_8 to C_{13} and C_{15} to C_{18} (Sigma-Aldrich, UK, purity ≥98.0%) and C_{14} (Tokyo Chemical Industry UK Ltd, purity 97.0%).

The filters were spiked with 30.0 μL of 30.0 μg mL^{-1} deuterated internal standards (dodecane-d$_{26}$, pentadecane-d$_{32}$, eicosane-d$_{42}$, pentacosane-d$_{52}$, triacontane-d$_{62}$, butylbenzene-d$_{14}$, nonylbenzene-2,3,4,5,6-d$_5$, biphenyl-d$_{10}$, p-terphenyl-d$_{14}$; Sigma-Aldrich, UK) for quantification and then immersed in methanol/dichloromethane (DCM) (1:1, v/v), and ultra-sonicated for 20 min at 20 °C. The extract

was filtered using a clean glass pipette column packed with glass wool and anhydrous Na$_2$SO$_4$, and concentrated to 100 μL under a gentle flow of nitrogen for analysis using GC x GC-ToF-MS. 1 μL of the extracted sample was injected in a split ratio 50:1 at 300 °C. The initial temperature of the primary oven (80 °C) was held for 2 min and then increased at 2 °C min^{-1} to 210 °C, followed by 1.5 °C min^{-1} to 325 °C. The initial temperature of the secondary oven (120 °C) was held for 2 min and then increased at 3 °C min^{-1} to 200 °C, followed by 2 °C min^{-1} to 300 °C and a final increase of 1 °C min^{-1} to 330 °C to ensure all species passed through the column. The transfer line temperature was 330 °C and the ion source temperature was 280 °C. Helium
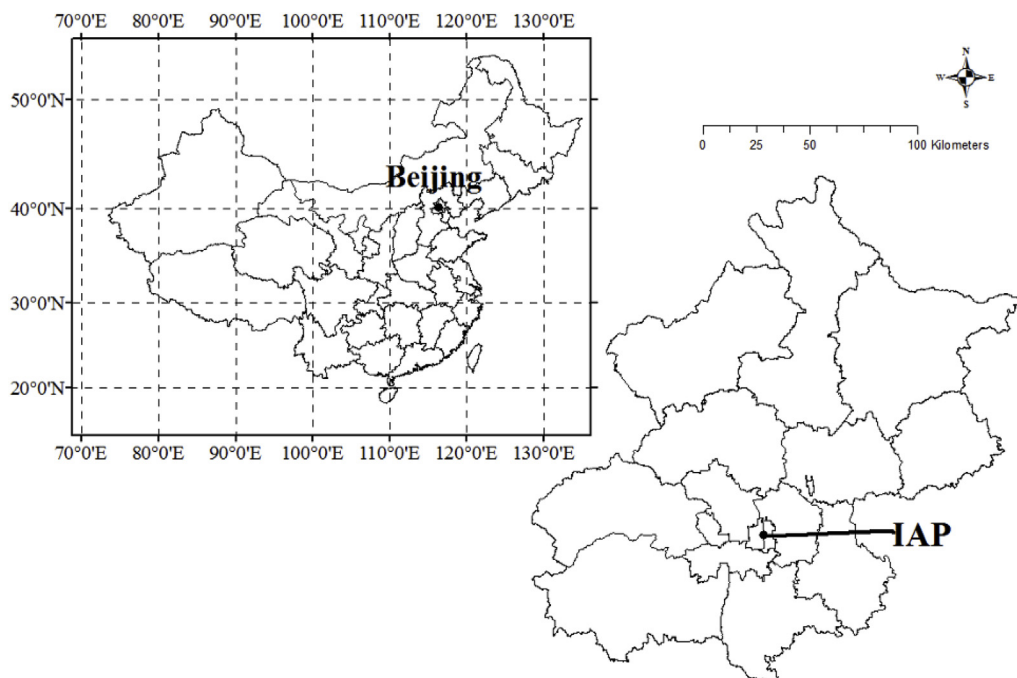

Fig. 1. Map of the sampling site. IAP: Institute of Atmospheric Physics, Chinese Academy of Sciences.

(99.999%) was used as the carrier gas at a constant flow rate of $1 \, mL \, min^{-1}$. Further details of the instrumentation and data processing methods is given by Alam and Harrison (2016) and Alam et al. (2016a,b).

Compound identification was based on the GCxGC-TOFMS spectral library, NIST mass spectral library and on co-injection with authentic standards. Compounds within the homologous series for which standards were not available were identified by comparing the retention time interval between homologues, and by comparison of mass spectra with the standards for similar compounds within the series, by comparison to the NIST mass spectral library, and by the analysis of fragmentation patterns.

The quantification for alkanes, aldehydes and 2-ketones was performed by the linear regression method using the seven-point calibration curves (0.05, 0.10, 0.25, 0.50, 1.00, 2.00, 3.00 $ng \, \mu L^{-1}$) established between the authentic standards/internal standard concentration ratios and the corresponding peak area ratios. The calibration curves for all target compounds were highly linear ($r^2 > 0.99$, from 0.991 to 0.997), demonstrating the consistency and reproducibility of this method. Limits of detection for individual compounds were typically in the range 0.001–0.08 $ng \, m^{-3}$ and 3-Ketones were quantified using the calibration curves for 2-ketones. This applicability of quantification of individual compounds using isomers of the same compound functionality (which have authentic standards) has been discussed elsewhere and has a reported uncertainty of 24% (Alam et al., 2018). Alkan-2-ones and alkan-3-ones were not well separated by the chromatography. These were separated manually using the peak cutting tool, attributing fragments at m/z 58 and 82 to 2-ketones and m/z 72 and 85 to 3-ketones.

Field and laboratory blanks were routinely analysed to evaluate analytical bias and precision. Blank levels of individual analytes were normally very low and in most cases not detectable. Recovery efficiencies were determined by analyzing the blank samples spiked with standard compounds. Mean recoveries ranged between 82 and 98%. All quantities reported here have been corrected according to their recovery efficiencies and blanks.

2.4. Determination of BC and OC

Black carbon (BC) was monitored simultaneously during the sampling period using an aethalometer (Model AE22, Magee Science). OC and EC were analyzed (a round punch of 0.538 cm^2) using the thermal–optical– transmittance (TOT) method (IMPROVE_A protocol, Desert Research Institute, USA).

2.5. Geochemical parameters and diagnostic ratios calculations

For the data analyses, molecular indicators of n-alkanes, such as carbon preference index (CPI), wax *n*-alkanes (WNA), wax *n*-alkanes ratios (WNA%), and carbon maximum number (C_{max}) were adopted for source-tracking and calculated by Eqs. (1) – (10), and all source indices utilized in this study are summarized in Table S1.

Carbon preference index (CPI), defined as the ratio of total odd number to even number compounds, had been widely used to evaluate the relative contribution of biogenic organics and anthropogenic emissions (Bray and Evans, 1961). The split CPI ranges were used to distinguish anthropogenic contributions (CPI_1) and higher plant wax input (CPI_2). C_{max}, the carbon number exhibiting the highest concentration, is usually used to distinguish biogenic from anthropogenic sources. The concentrations of wax n-alkanes (WNA%) have been used to estimate the relative contributions of biogenic versus anthropogenic sources (Simoneit, 1985), while PNA% (equal to 100% - WNA%) stands for the n-alkanes from petrogenic sources. The concentrations of the wax *n*-alkanes are calculated by subtraction of the average of the next higher and lower even carbon numbered homologues, taking as zero the negative values of C_n.

$$For \; n-alkanes; \; CPI = \frac{1}{2}\left(\frac{\sum odd(C_{11}-C_{35})}{\sum even(C_{10}-C_{34})} + \frac{\sum odd(C_{11}-C_{35})}{\sum even(C_{12}-C_{36})} \right) \tag{1}$$

$$For \; n-alkenes; \; CPI = \frac{1}{2}\left(\frac{\sum odd(C_{13}-C_{25})}{\sum even(C_{12}-C_{24})} + \frac{\sum odd(C_{13}-C_{25})}{\sum even(C_{14}-C_{26})} \right) \tag{2}$$

$$For \; n-alkanals; \; CPI = \frac{\sum odd(C_9-C_{29})}{\sum even(C_8-C_{28})} \tag{3}$$

$$For \; n-alkan-2-ones: \; CPI = \frac{\sum odd(C_9-C_{31})}{\sum even(C_8-C_{30})} \tag{4}$$

$$For \; n-alkan-3-ones: \; CPI = \frac{1}{2}\left(\frac{\sum odd(C_9-C_{29})}{\sum even(C_8-C_{28})} + \frac{\sum odd(C_9-C_{29})}{\sum even(C_{10}-C_{30})} \right) \tag{5}$$

$$For \; n-alkanes: \; CPI_1 = \sum (C_{11}-C_{25})/\sum (C_{10}-C_{24}) \tag{6}$$

$$For \; n-alkanes: \; CPI_2 = \frac{1}{2}\left(\frac{\sum odd(C_{27}-C_{35})}{\sum even(C_{26}-C_{34})} + \frac{\sum odd(C_{27}-C_{35})}{\sum even(C_{28}-C_{36})} \right) \tag{7}$$

$$WNA = C_n - \left(\frac{C_{n-1}+C_{n+1}}{2} \right) \tag{8}$$

$$WNA\% = \frac{\sum WNA_{Cn}}{\sum NA_{Cn}} \times 100\% = \sum \left(C_n - \left(\frac{C_{n-1}+C_{n+1}}{2} \right) \right)/\sum C_n \times 100\% \tag{9}$$

$$PNA\% = 100\% - WNA\% \tag{10}$$

3. Results and discussion

3.1. General aerosol characteristics

A haze episode was defined as having a $PM_{2.5}$ concentration exceeding 75 $\mu g \, m^{-3}$ (24 h average) according to the National Ambient Air Quality Standards of China (NAAQS) released in 2012 by the Ministry of Environmental Protection (MEP) of the People's Republic of China; 33 samples were separated into non-haze (13) and haze (20) days. The average $PM_{2.5}$ concentration of the sampling campaigns was 95.4 ± 68.5 $\mu g \, m^{-3}$, and this is more than two times the Chinese annual $PM_{2.5}$ standard (35 $\mu g \, m^{-3}$) (Fig. 2). In addition, the average $PM_{2.5}$ concentration was 141 ± 51.9 $\mu g \, m^{-3}$ during all haze episodes, which is four times greater than the average of the non-haze period (35.3 ± 21.0 $\mu g \, m^{-3}$).

Haze days are characterized by stagnant air conditions with high relative humidity (RH), and weak wind speeds, which are unfavourable for particle dispersion. Such an obvious trend in this study highlights a significant impact of meteorological conditions, the wind and temperature during the haze and non-haze days were 0.94 and 1.44 m/s, 6.07 and 4.0 °C, respectively. However, the relative humidity during haze episodes (56.3%) was slightly higher than the non-haze periods (39.8%). The concentrations of gaseous pollutants SO_2, NO_x, and CO were simultaneously elevated with the increase of $PM_{2.5}$ concentrations, whereas O_3 concentration presented an opposite trend to $PM_{2.5}$ concentrations (Shi et al., 2018).

Source apportionment results (Liu et al., 2018) have shown that the average contribution of liquid fuels (e.g., vehicle emissions) to BC was around 50% on non-haze air days in Beijing. During pollution episodes, solid fuel sources including coal combustion and biomass burning were the predominant sources, accounting for 61–83% of BC. The concentrations of BC were simultaneously determined during the
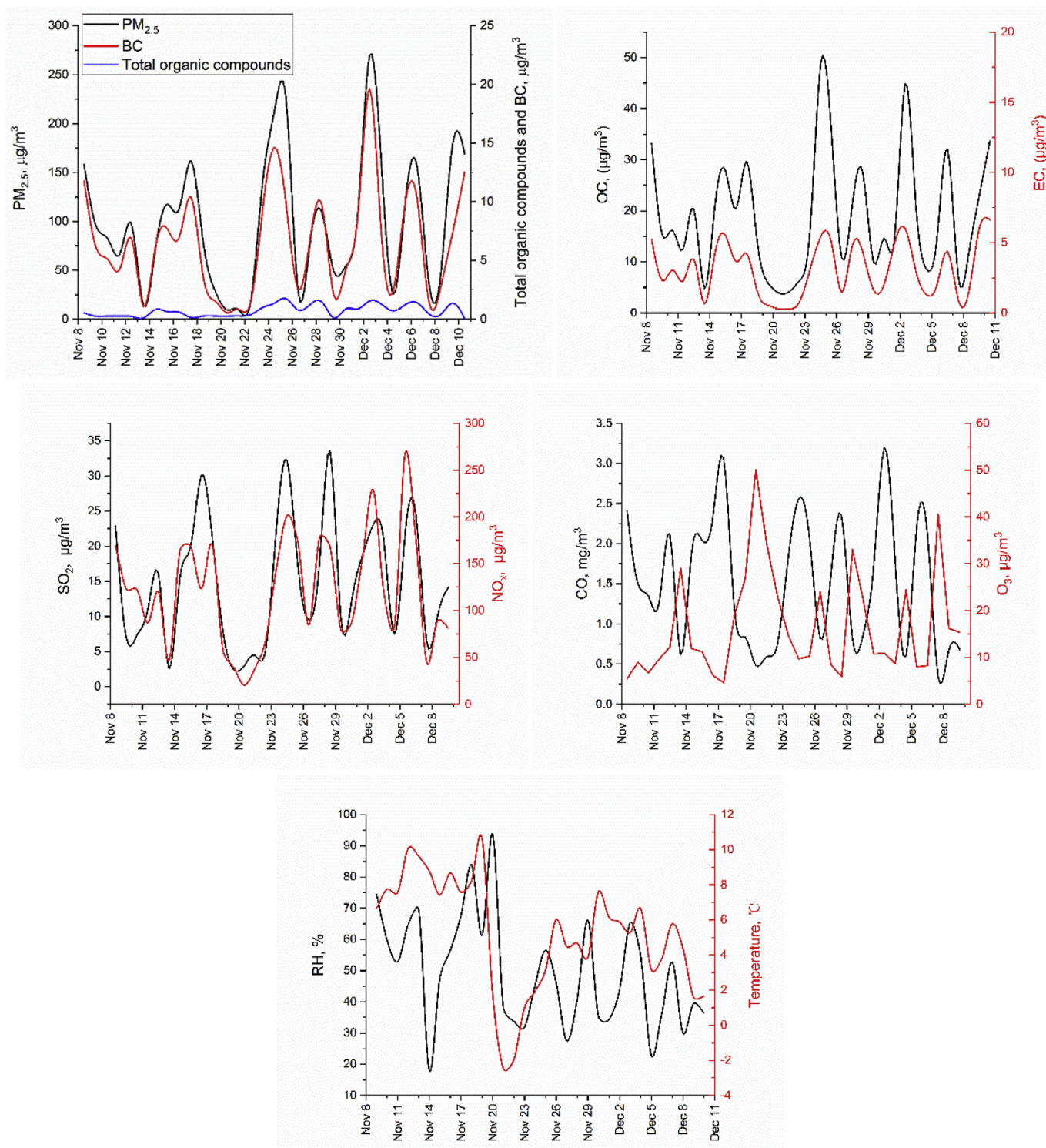
Fig. 2. Variations of particulate matter concentrations (PM$_{2.5}$) together with main meteorological variables, typical air pollution parameters and total mass concentration of 115 organic compounds during the sampling period.

campaigns. The daily concentrations of BC ranged from 0.56 to 19.6 µg m^{-3} with an average of 6.54 µg m^{-3}, and this was comparable with the results of the study conducted in winter 2015 in Beijing (Liu et al., 2018) with an average of 5.31 µg m^{-3}. Additionally, the haze days had higher BC concentrations (average 9.21 µg m^{-3}) and were more than three times higher than the non-haze air period (average 2.42 µg m^{-3}).

Food cooking is a major source of PM$_{2.5}$ emissions (Abdullahi et al.,

2013; Wu et al., 2018), and studies in China have attributed substantial amounts (5.8–20.2%) of PM$_{2.5}$ to this source (Wu et al., 2018). Cooking emits a large range of organic compounds, which include alkanes, alkanals and alkanones. According to data reported by Zhao et al. (2007), mean concentrations of compound groups arising from Chinese cooking are n-alkanes, 1880 ng mg^{-1}; n-alkanals, 3440 ng mg^{-1} and n-alkanones, 2440 ng mg^{-1}. The maximum carbon number abundances are reported as C$_{23}$ for n-alkanes, C$_9$ for alkanals and C$_{16}$ for alkanones,

although the studies do not measure across the full range of molecular weights of our study (Abdullahi et al., 2013). It seems likely that cooking emissions contribute to the measured concentrations, but on the basis of the within-particle concentrations listed above, the contribution to the concentrations of individual alkanes, alkanals or alkanones appear likely to be quite small.

Wu et al. (2018) report the results of a number of published studies from China in which receptor modelling has been applied to source apportionment of organic aerosol. The sources included are biomass burning, coal combustion, gasoline exhaust, diesel exhaust and cooking. These are discussed where relevant in relation to the measured compounds.

3.2. Aliphatic hydrocarbons

The concentration of organic matter (OM) was be estimated as $30.2 \, \mu g \, m^{-3}$ using an OC concentration ($18.9 \, \mu g \, m^{-3}$) multiplied by a factor of 1.6, typical of aged aerosol (Turpin and Lim, 2001). More than one hundred aliphatic hydrocarbons were identified in this study (Table S2), including saturated and unsaturated aliphatic hydrocarbons (27 n-alkanes, 15 n-alkenes), and 79 aliphatic carbonyl compounds (22 n-alkanals, 24 n-alkan-2-ones, 23 n-alkan-3-ones), 9 furanones and phytone. The total concentrations of identified organic compounds ranged from 110 to $1783 \, ng \, m^{-3}$ with the average of $744 \pm 510 \, ng \, m^{-3}$, accounting for 0.36–5.91% (average 2.47%) of OM.

3.2.1. n-Alkanes

n-Alkanes, ranging from C_{10} to C_{36}, were abundant in all $PM_{2.5}$ samples. The daily total concentration of compounds was estimated from the sum of homologue compounds measured in the fine aerosols and is shown as Σ. The Σ n-alkanes (C_{10}-C_{36}) ranged from 42.4 to $1241 \, ng \, m^{-3}$ with an average $450 \pm 316 \, ng \, m^{-3}$, and this was comparable with the results of the previous study conducted in the winter of 2013 in Beijing ($426 \, ng \, m^{-3}$) (Kang et al., 2018). Additionally, the average Σ n-alkanes was $577 \, ng \, m^{-3}$ during haze episodes, more than twice that of the non-haze period ($264 \, ng \, m^{-3}$). Table 1 presents the comparison of concentrations and diagnostic parameters with other cities around China. Such comparisons must be viewed with caution as site location, seasonal variations in emissions, and meteorological factors influence airborne concentrations, and these differ between datasets from the various studies. Table 1 shows that the north China cities (Beijing and Tianjin) have higher average concentrations of n-alkanes than other cities, especially in the winter heating season while the cities located in the south of China are probably more impacted by biogenic emissions. In addition, the large metropoles, including the Beijing-Tianjin-Hebei region and Yangtze River Delta of China, have higher regional concentrations of n-alkanes, implying significant contributions from primary emission sources.

The concentrations of n-alkanes at the Beijing IAP site were substantially lower than measured in our previous studies conducted at Regent's University (RU) in London. The two sites (IAP and RU) have similar conditions as both are close to the city centre and affected by nearby major highways. The Σ n-alkanes (C_{11}-C_{36}) at RU ranged from 103 to $1741 \, ng \, m^{-3}$ with an average of $737 \pm 441 \, ng \, m^{-3}$. Far higher concentrations are measured at the nearby Marylebone Road street canyon site indicating a substantial contribution from road traffic.

The correlations between individual n-alkanes and $PM_{2.5}$ in Beijing have been calculated in the non-haze and haze periods in order to assess the emission sources, and the regression equations are detailed in Table S3. The correlations (r^2) between individual n-alkanes (C_{24}-C_{31}) and $PM_{2.5}$ ranged from 0.27 to 0.51 during the non-haze days, whereas the correlation of n-alkanes (C_{30}-C_{36}) and $PM_{2.5}$ were in the range of 0.32–0.55 in the haze periods. The results are quite consistent with the correlations between BC and individual n-alkanes. The n-alkanes (C_{22}-C_{31}) have fair correlations ($r^2 = 0.57$ (average), range: 0.31–0.80) with BC on the non-haze days, whereas the n-alkanes (C_{30}-C_{36}) and BC

showed less strong correlations ($r^2 = 0.46$ (average), range: 0.30–0.55) during the haze periods (Table S4). These moderate correlations suggest that the high molecular weight n-alkanes arise in part from sources contributing to elevated $PM_{2.5}$ concentrations. The difference in correlation behaviour in the non-haze and haze periods may be influenced by a number of factors, including different sources, dispersion and deposition processes. The observed correlations may indicate local vehicular exhaust and coal combustion as major sources in the different periods. There may also be a large contribution from secondary aerosol during the haze periods. A sequence of studies that have measured levoglucosan indicate a steady decline of mean concentrations from 1403 to $189 \, ng \, m^{-3}$ in the period of 2003–2014 in the winter in Beijing (He et al., 2006; Zhang et al., 2008; Cheng et al., 2013; Yan et al., 2015; Kang et al., 2018). The latter study (Kang et al., 2018) reported good correlations between levoglucosan and HMW alkanes ($r^2 = 0.77$) in Beijing in the winter of 2013, which were attributed to biomass burning in the area around Beijing.

Anthropogenic sources, including fossil fuel burning and vehicular emissions, usually consist mainly of low and medium chain length (MW $< C_{25}$) n-alkanes, while biomass burning or plant waxes are important contributors to the n-alkanes with longer chain length (HMW $> C_{25}$) (Simoneit et al., 2004). The predominance of odd carbon number compounds is another characteristic of n-alkanes from biomass burning or plant waxes (Simoneit et al., 2004). The n-alkanes (C_{20}-C_{31}) were the most abundant homologues (Fig. 3), accounting for approximately 83.0% of the Σn-alkanes. The previous studies (Hong et al., 2017; Li et al., 2013; Han et al., 2018; Xu et al., 2013) reported similar distributions to our data in many cities of China (Beijing, Shanghai, Guangzhou, Nanjing, Ningbo, and Jiujiang) with abundant n-alkanes in the range of C_{19}-C_{25}, C_{25}-C_{34} and C_{27}-C_{29}. A small odd carbon number predominance (C_{27}, C_{29}, and C_{31}) was observed in the samples, indicating an influence from biomass burning and plant waxes. The C_{max} of n-alkane homologues in our data was at C_{25} ($45.6 \, ng \, m^{-3}$), followed by C_{23} ($44.6 \, ng \, m^{-3}$), C_{22} ($44.4 \, ng \, m^{-3}$), C_{24} ($43.6 \, ng \, m^{-3}$), C_{26} ($41.4 \, ng \, m^{-3}$) and C_{27} ($38.6 \, ng \, m^{-3}$) (Fig. 3). Coal smoke particulate matter (Oros and Simoneit, 2000) is characterized by n-alkanes (C_{16}-C_{34}) with C_{max} at C_{29}, as well as a peak at C_{25} while vehicle emissions are characterized by n-alkanes (C_{14}-C_{29}) with C_{max} at C_{18} and C_{25} for gasoline vehicles (Schauer et al., 2002) and C_{20} for medium-duty diesel trucks (Schauer et al., 1999b). The higher concentration of n-alkanes in the range C_{22}-C_{26} suggests significant contributions from anthropogenic sources to n-alkanes in Beijing city, probably including diesel and gasoline vehicle emissions and coal combustion. Surprisingly, a peak at C_{11} was observed which is hard to explain from the published literature. However, this finding was reported in winter samples from Shanghai (Lyu et al., 2017) and attributed to significant anthropogenic inputs from increased vehicular emissions.

The average CPI value obtained for C_{10} to C_{36} n-alkanes was 1.27, implying a predominant contribution from fossil carbon sources in Beijing. The low CPI value is in good agreement with those reported in Beijing and other urban aerosols from China (Ren et al., 2016; Han et al., 2018; Xu et al., 2013; Yadav et al., 2013; Feng et al., 2006) (Table 1). The value of CPI_1 (1.37) indicated a substantial impact of human activities, and similar results were found in samples from the Yangtze River Delta (Hong et al., 2017), and the higher CPI_2 (1.64) value showed a weak contribution from plant waxes and other biogenic sources. The average contribution of plant wax n-alkanes to the total n-alkanes (WNA%) was 14.6%, implying that 85.4% of n-alkanes originated from anthropogenic sources. The contribution of plant waxes to the total n-alkane loadings was relatively small and comparable to the study conducted in the winter of 2013 at the IAP site which showed 11.6% (Kang et al., 2018), but far lower than the 41% reported by Li et al. (2013) for samples collected in the 2006 winter in the Beijing urban area. This indicates that plant wax is not currently a major source of the winter-time high molecular weight n-alkanes at the IAP site. Biomass burning activities around Beijing have decreased significantly
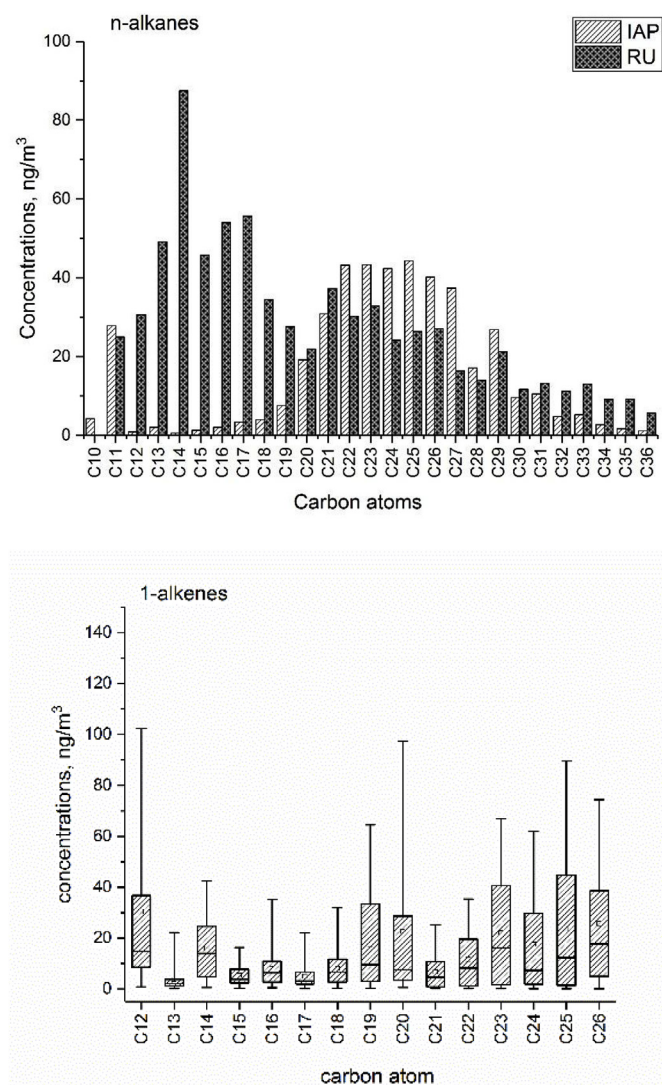
Fig. 3. Carbon number distributions and mass concentrations of PM$_{2.5}$-bound n-alkanes and n-alkenes at IAP (Beijing) and RU (London).

as strict air pollution control measures have been implemented in recent years, as evidenced by previous studies which demonstrated that the concentrations of levoglucosan gradually decreased from winter 2003 to 2014, as referred to above. Kang et al. (2018) reported a correlation ($r^2 = 0.77$) between levoglucosan and HMW alkanes in Beijing in the winter of 2013, attributed to biomass burning in the area around Beijing.

3.2.2. n-Alkenes

Alkenes constitute a significant class of volatile organic compounds present in the atmosphere of Beijing (Duan et al., 2008; Yang et al., 2018; Wu et al., 2017). The high rate coefficients of n-alkenes for reaction with ozone (O_3) and hydroxyl radicals (OH) usually result in lifetimes ranging from a few minutes to 1–2 days and the reaction products can lead to SOA formation (Matsunaga et al., 2009). The alkenes of lower molecular weight (C_2-C_5) have been identified in the samples from Beijing (Duan et al., 2008) with concentrations ranging from 1.24 to 6.13 μg m^{-3}, which were far higher than the long-chain 1-alkenes identified in the present study. The concentrations of 1-alkene homologues with carbon numbers from C_{12} to C_{26} ranged from 3.82 to 31.5 ng m^{-3}, and the average Σ n-alkenes was 210 ± 165 ng m^{-3} during the sampling period. Additionally, the average Σ n-alkenes concentration was 252 ng m^{-3} during all haze episodes, which was 1.8

times the 143 ng m^{-3} of the non-haze days.

The n-alkenes were probably derived from the dehydration of n-alkanols and cracking of n-alkanes during incomplete coal and biomass combustion (Simoneit, 2002). Oros and Simoneit (2000) reported that coal smoke particulate matter is characterized by n-alkenes (C_{14}-C_{28}) with C_{max} at C_{28}, and the average CPI is 0.78 (0.9 for lignite, 0.1 for brown coal, 1.2 for sub-bituminous and 0.9 for bituminous coal). Wood burning (Simoneit et al., 2000) is characterized by n-alkenes (C_{18}-C_{31}) with C_{max} at C_{24} and CPI 0.35. The n-alkene homologues determined in the present studies represented a range from C_{12} to C_{26} with the C_{max} at C_{12} (31.5 ng m^{-3}), followed by C_{26} (27.6 ng m^{-3}). Probably due to the high chemical reactivities of n-alkenes, poor correlations between individual n-alkenes and PM$_{2.5}$ and BC were obtained with average values of $r^2 = 0.16$ (0.02–0.36) and $r^2 = 0.12$ (0.00–0.25), respectively. The distributions of n-alkenes were dominated by the high molecular weight compounds (C_{23}-C_{26}) with CPI 0.75 (Fig. 3), which are suggestive of significant contributions from coal combustion.

Although coal burning has recently been banned in urban Beijing, residential coal combustion continues in the area around Beijing and makes a contribution to the PM. The studies of Xu et al. (2018) demonstrate that residential coal combustion made a contribution (21%) to the PM$_{2.5}$ in a southwestern suburb of Beijing during the winter of 2016. Similar results were found by Fan et al. (2018) who reported that combustion of coal, vehicle emissions, residential emissions and biomass combustion are the major contributors to atmospheric particulates in Beijing.

3.3. Aliphatic carbonyl compounds

In all, 69 aliphatic carbonyl compounds were identified in the samples. The time series of particle-bound n-alkanals, n-alkan-2-ones, and n-alkan-3-ones are plotted in Fig. 4. It is clear that the concentrations of carbonyl compounds show substantial variability, and the n-alkan-3-ones have lower concentrations than the n-alkanals and n-alkan-2-ones. Carbonyl compounds show a sudden increase from 23 November 2016 which may be caused by the local meteorological conditions and accumulation during the formation of haze episodes. The daily sum of aliphatic carbonyls, ΣAC, ranged from 8.87 to 164 ng m^{-3}, accounting for 0.02–0.46% of OM. The average ΣAC was 75.8 ng m^{-3} during all haze days, approximately double the 39.5 ng m^{-3} of the non-haze air period. The correlation (r^2) between Σ n-alkanes and daily total aliphatic carbonyls (ΣAC) was high (0.85) (Fig. 4), suggesting that a common primary source input was a major contributor. Carbonyls identified in this study differ in some aspects from those previously reported in samples collected from Regent's University (RU) in London (Lyu et al., 2018), presenting wide ranges of carbon numbers and lower concentrations. A detailed comparison of carbonyl compounds between IAP (Beijing) and RU (London) is shown in Figs. 5 and 6. Table 2 presents the CPI and C_{max} of particle-bound carbonyl compounds determined in the current and other studies.

Carbonyl compounds with high carbon numbers presented good correlations with PM$_{2.5}$ during the haze episodes, with the average $r^2 = 0.45$ (0.12–0.73) for n-alkanals (C_{18}-C_{29}), $r^2 = 0.50$ (0.26–0.63) for n-alkan-2-ones (C_{16}-C_{31}), and $r^2 = 0.38$ (0.22–0.51) for n-alkan-3-ones (C_{16}-C_{30}), respectively (Table S3). The good correlations suggest that the higher molecular weight aliphatic carbonyls and fine particulate matter share similar or related sources during the haze formation process. On the other hand, the carbonyl compounds with low molecular weight are probably mainly emitted from vehicle exhaust or formed from OH oxidation of n-alkanes as poor correlations were obtained with the fine particulate matter on the non-haze days.

3.3.1. n-Alkanals

The n-alkanal homologues with carbon number from C_8 to C_{29} were identified in the Beijing samples, and the individual compound atmospheric concentrations were in the range of 0.53–8.91 ng m^{-3} with an
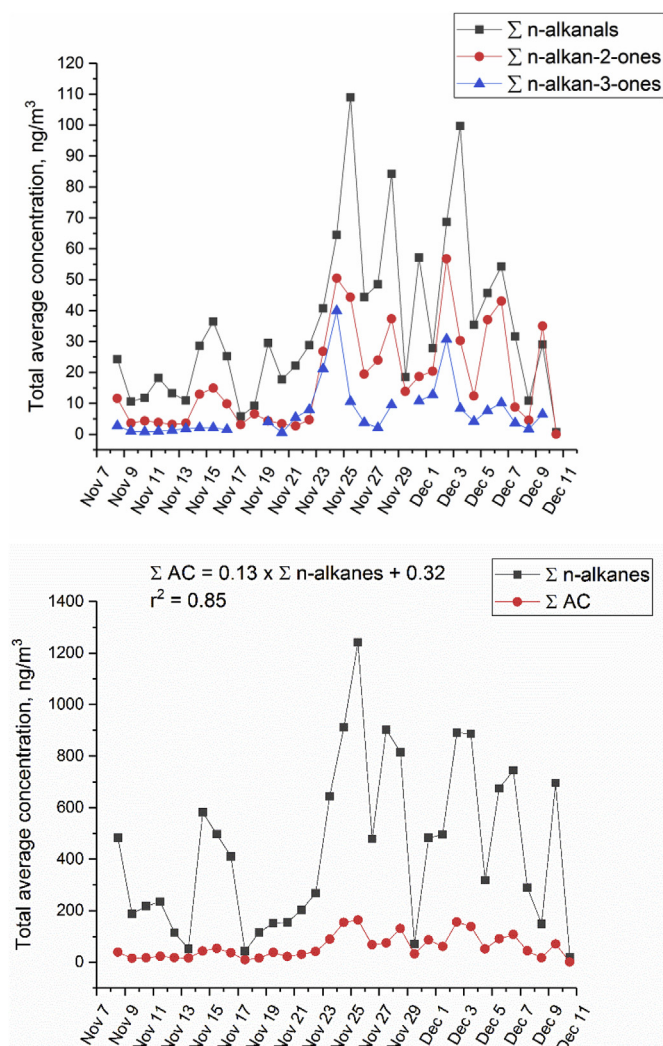
Fig. 4. Time series of Σ 1-alkanals, Σ n-alkan-2-ones and Σ n-alkan-3-ones (Σ stands for the summed daily total concentration of homologues) (top panel) and the daily variation of Σ n-alkanes and Σ AC (daily total aliphatic carbonyls, i.e. the sum of the Σ 1-alkanals, Σ n-alkan-2-ones and Σ n-alkan-3-one) (lower panel) at the Beijing IAP site. The regression equation between Σ n-alkanes and Σ AC is shown in the figure.
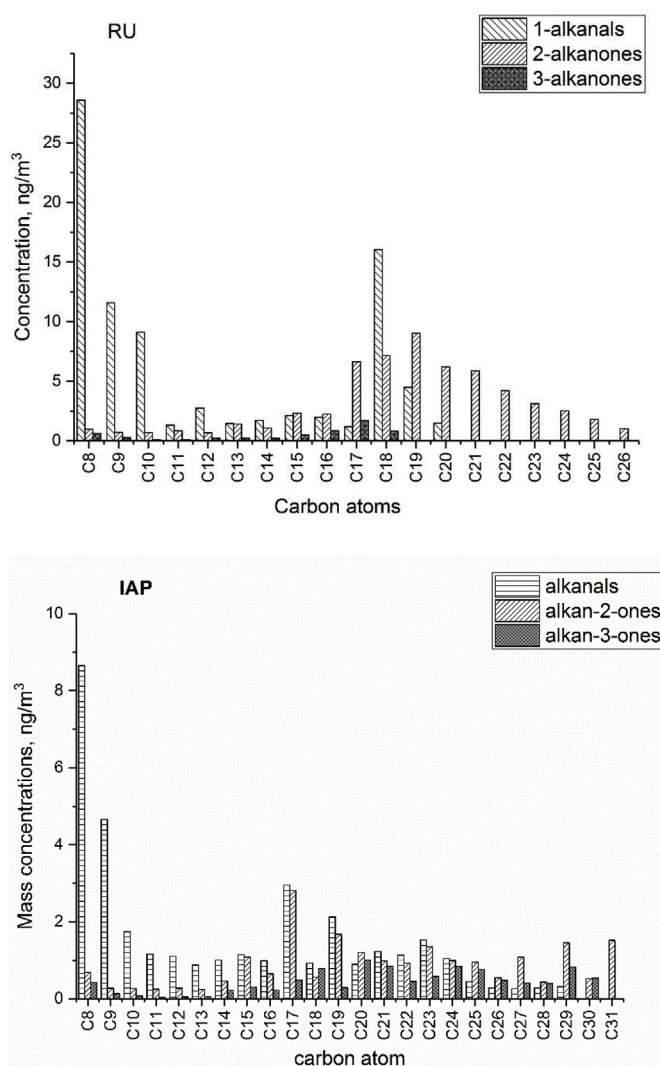

Fig. 5. The molecular distribution of carbonyl compounds, including 1-alkanals, n-alkan-2-ones and n-alkan-3-ones, in London (Regent's University)-upper panel, and Beijing (IAP site)-lower panel.

average of $1.75\,ng\,m^{-3}$ (Table S2), which was slightly higher than those (C_{10}-C_{32}, 0.4–$2.6\,ng\,m^{-3}$) reported in rural and urban samples from Heraklion, Crete (Gogou et al., 1996). This finding was quite different from the observations of C_8-C_{20} in samples collected in winter in RU in London where high concentrations in the range of 1.20–$28.6\,ng\,m^{-3}$ with an average of $6.44\,ng\,m^{-3}$ were observed. In addition, the average Σ n-alkanals in Beijing was up to $36.3\,ng\,m^{-3}$, accounting for 63.5% of the total measured aliphatic carbonyls, which was lower than the $82.6\,ng\,m^{-3}$ measured at RU in London. Fig. 5 shows the molecular distributions of n-alkanals, exhibiting a bimodal distribution with the C_{max} at C_8 ($8.91\,ng\,m^{-3}$) and the secondary peak at C_{17} ($3.75\,ng\,m^{-3}$), with a low CPI (1.00) (Table 2). Andreou and Rapsomanikis (2009) reported the C_{max} as C_{15} or C_{17} in Athens and attributed this to the oxidation of n-alkanes. However, a C_{max} at C_{26} or C_{28} was observed in Heraklion (Gogou et al., 1996), suggestive of biogenic input. The homologue distribution and CPI of n-alkanals in this study differed from Athens and Heraklion, and demonstrated weak biogenic input and a strong impact of anthropogenic activities in the Beijing samples. The hypothesis was supported by the similar ratios of n-alkanes/n-alkanals (C_{12}-C_{18}) with the same carbon atom numbers in both Beijing and diesel engine exhaust studies (Fig. 7a). The details of

the engine set up and exhaust sampling system are given elsewhere (Alam et al., 2016a). The latest studies (Lyu et al., 2018) indicate that vehicle emissions are the main source of n-alkanals (C_8-C_{20}) at RU in London, with the C_{max} at C_8 and the secondary peak at C_{18} (Fig. 6). The ratios of n-alkanes/n-alkanals (C_{13}-C_{18}) with the same carbon numbers at RU, IAP and in the engine exhaust studies were in the ranges of 2.15–50.6, 0.80–4.35 and 0.52–7.6, respectively (Fig. 7a). The similar n-alkane/n-alkanal ratios from IAP and engine studies suggest that atmospheric n-alkanals with lower molecular weight in the two metropolitan regions mainly arise from vehicle emissions, although in London diesel dominates the light-duty fleet, while gasoline is dominant in Beijing, so this inference is highly tentative.

The n-alkanals (C_{19}-C_{29}) with high molecular weight showed medium correlations with BC during haze periods and poor correlations on non-haze days, with the average (and range) $r^2 = 0.39$ (0.18–0.77) and 0.10 (0.00–0.33), respectively (Table S4). This difference is suggestive of a common source of long-chain n-alkanals (C_{19}-C_{29}), with BC contributing to haze formation. Furthermore, good correlations were obtained between high molecular weight n-alkanes and n-alkanals (C_{19}-C_{29}) with the same carbon numbers during haze episodes (Table S5), with average $r^2 = 0.57$ (0.36–0.82), strongly indicating closely related sources of both classes of compound or formation of alkanals from alkane oxidation.
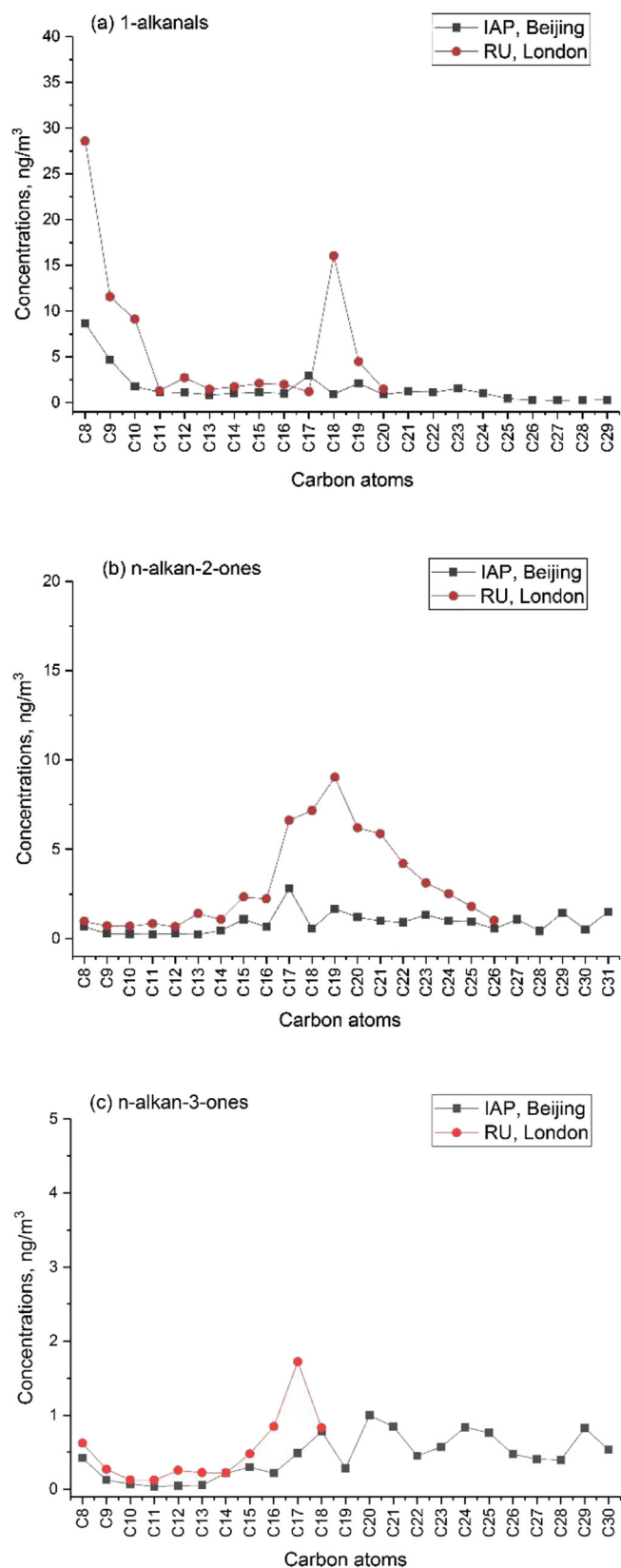
Fig. 6. The comparisons of molecular distribution of carbonyl compounds (a) 1-alkanals, (b) n-alkan-2-ones and (c) n-alkan-3-ones between IAP (Beijing) and RU (London).

3.3.2. n-Alkan-2-ones

The n-alkan-2-one homologues have been previously identified in organic aerosol samples from rural and urban areas, and were considered to originate mainly from atmospheric oxidative processes and biogenic inputs (Gogou et al., 1996; Andreou and Rapsomanikis, 2009; Zhang et al., 2015). The latest studies (Lyu et al., 2018) reported n-alkan-2-ones (C_8-C_{24}) at Regent's University in London with Σ n-alkan-2-ones from 16.5 to 112 ng m^{-3}, which were considered probably to be formed via the OH-initiated heterogeneous reactions of n-alkanes. In China, coal combustion should be considered as another important source of n-alkan-2-ones as these compounds have been identified in coal smoke particulate matter (Oros and Simoneit, 2000). Coal smoke particulate matter is characterized by n-alkan-2-ones with chain lengths of C_{13}-C_{33}, and the CPI values for lignite (C_{max} at C_{29}), brown (C_{max} at C_{29}), sub-bituminous (C_{max} at C_{29}) and bituminous (C_{max} at C_{27}) coal were 1.2, 1.9, 1.7, and 0.9, respectively.

The concentrations of n-alkan-2-one homologues (C_8-C_{31}) ranged from 0.24 to 2.81 ng m^{-3} with C_{max} at C_{17} (Fig. 5), and the average individual concentration (0.88 ng m^{-3}) (Table S2) was lower than 5.4 ng m^{-3} measured in Athens (Andreou and Rapsomanikis, 2009) and 3.1 ng m^{-3} measured at Regent's University. This finding is slightly higher than the five sampling sites of the CARBOSOL project (Oliveira et al., 2007) with average concentrations ranging from 0.15 ng m^{-3} (C_{17-29}) to 0.6 (C_{16}-C_{31}), while lower than one site 3.35 ng m^{-3} (C_{14}-C_{31}). In addition, the average Σ n-alkan-2-ones was 18.0 ng m^{-3}, accounting for 27.5% of total identifiable aliphatic carbonyls. The CPI value for n-alkan-2-ones (1.83) (Table 2) was higher than that measured in previous studies in Athens (Andreou and Rapsomanikis, 2009) (1.49), Heraklion (Gogou et al., 1996) (0.8–1.4) and London (0.57–1.23), but this was not as high as expected for appreciable biogenic input, indicating that the sources from anthropogenic activity and OH oxidation of n-alkanes are predominant. Fig. 6 shows the distribution and concentration comparisons of n-alkan-2-ones between IAP (Beijing) and Regent's University (London). The average Σ n-alkan-2-ones measured at RU was 58.5 ng m^{-3} with C_{max} at C_{19} (9.0 ng m^{-3}), approximately three times greater than 18.0 ng m^{-3} measured in the Beijing samples. This substantial difference between IAP and RU is probably caused by higher emissions in London.

Good correlations between individual n-alkan-2-ones (C_{16}-C_{31}) and BC were obtained during the haze episodes, with the average $r^2 = 0.48$ (0.13–0.67) (Table S4), suggesting that coal combustion was the main source of high molecular weight n-alkan-2-ones. Surprisingly the C_{max} at C_{17} in Beijing was not as high as expected for the higher molecular weight n-alkan-2-ones on the haze days; the probable reason was that the n-alkan-2-ones with medium length chain were mainly contributed by mixed sources, including coal combustion, vehicular exhaust and OH oxidation of n-alkanes. It is notable that the n-alkan-2-ones with carbon number around C_{18} (C_{17}-C_{20}) have medium correlations with BC relative to the other compounds during the non-haze days, which were probably linked to vehicle exhaust input (Table S4). The strong correlations between individual n-alkan-2-ones and BC on the haze days may be indicative of vehicle emissions and coal combustion as another source (Table S4).

3.3.3. n-Alkan-3-ones

The aliphatic n-alkan-3-ones were first identified in the particle samples collected in London with carbon numbers from C_8-C_{19} (Lyu et al., 2018). The n-alkan-3-one homologues with carbon numbers C_8-C_{31} were identified at IAP, and the Σ n-alkan-3-ones ranged from 0.57 to 40.0 ng m^{-3} with an average of 7.44 ng m^{-3} (Fig. 5). The average Σ n-alkan-3-one concentration has the same order of magnitude as Regent's University, London (RU, 5.65 ng m^{-3}) and far lower than the roadside MR site in London (39.4 ng m^{-3}). The distribution and concentration comparisons of n-alkan-3-ones between Beijing and RU are shown in Fig. 6. In addition, a low CPI of n-alkan-3-ones (0.92) was obtained, and C_{max} was at medium chain length (C_{20}) with

Table 2

Carbon preference index (CPI) and C_{max} of n-alkanals, n-alkan-2-ones, and n-alkan-3-ones in published studies.

| Location	Sampling period	n-alkanals		n-alkan-2-ones		n-alkan-3-ones		Reference
Sampling sites		CPI	C_{max}	CPI	C_{max}	CPI	C_{max}	
IAP, Urban, Beijing	9 Nov - 11 Dec (2016)	1.00	C_8	1.83	C_{17}	0.92	C_{20}	Present study
RU, Regent's University, London	24 Jan – 20 Feb (2017)	0.41	C_8	0.99	C_{20}	1.26	C_{17}	Lyu et al. (2018)
Athens, Athinas St.	August	1.49	C_{15}, C_{17}	1.09	C_{18}, C_{21}, C_{19}			Andreou and Rapsomanikis et al. (2009)
Urban roadside	March			3.26	C_{21}, C_{19}, C_{20}			
Athens, AEDA, Urban, 20 m above ground	March			2.41	C_{19}, C_{18}, C_{20}			Andreou and Rapsomanikis et al. (2009)
Heraklion, Greece Urban 15 m above ground	Spring/summer	0.8–1.4	C_{26}, C_{28}	1.3–1.8	C_{23}, C_{29}, C_{31}			Gogou et al., 1006
Vancouver, Canada Roadway tunnel				1.33	C_{17}, C_{19}			Cheng et al. (2006)
Aveiro, Portugal	Summer		C_{22}, C_{23}, C_{26}		C_{26}, C_{28}, C_{30}			Oliveira et al. (2007)
Suburban	Winter							
K-Puszta, Hungary	Summer		C_{24}, C_{26}, C_{28}		C_{24}, C_{26}, C_{28}			Oliveira et al. (2007)
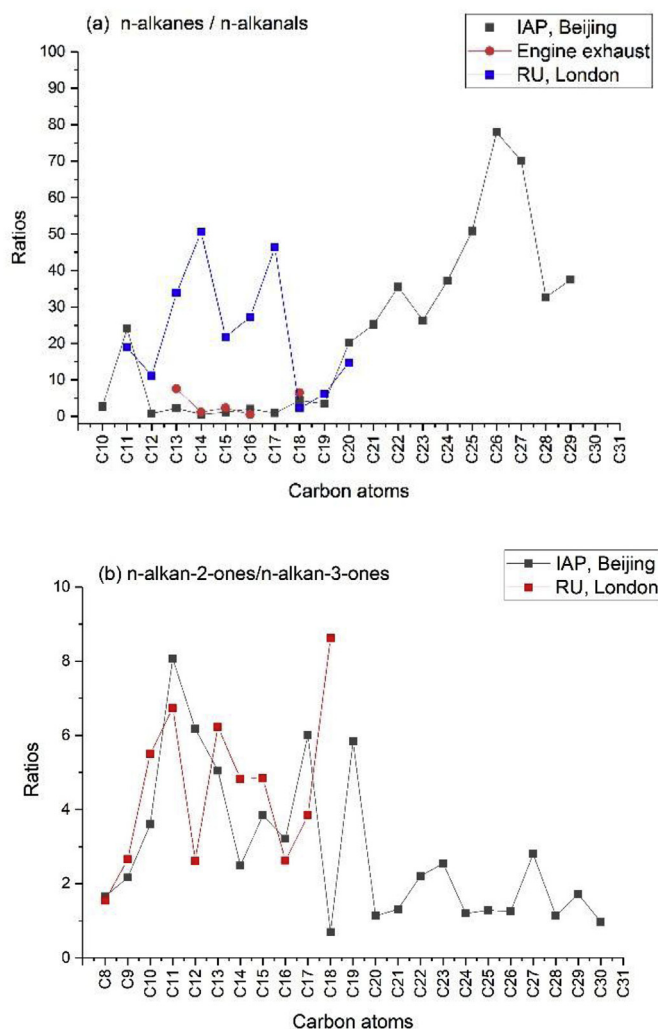
Fig. 7. The comparison of ratios of (a) n-alkanes/alkanals, (b) n-alkan-2-ones/n-alkan-3-ones with same carbon numbers between IAP (Beijing) and RU (London). The (a) n-alkanes/n-alkanals include the results from diesel engine studies.

concentration 1.06 ng m^{-3}, unlike the RU site in London where CPI was 1.30 with C_{max} at C_{17}. Strong correlations r^2 = 0.57 (0.13–0.77) of n-alkan-3-ones (C_{17}-C_{30}) and BC were observed during the haze days,

suggestive that the high molecular weight n-alkan-3-ones and BC probably have similar or related sources, although the aliphatic n-alkan-3-ones have not been reported in published primary source profiles.

Chamber studies (Zhang et al., 2015) have demonstrated that n-alkan-2-ones and n-alkan-3-ones are abundant functional and fragmental OH oxidation products of n-alkanes, and 1-undecanal, hexan-3-one, octan-3-one, heptan-2-one, nonan-2-one and decan-2-one have been identified from the chamber studies of dodecane oxidation (Schilling Fahnestock et al., 2015). Studies of the OH oxidation of n-alkanes (Kwok and Atkinson, 1995; Ruehl et al., 2013) have demonstrated that the distribution of first-generation carbonyl products depends strongly upon whether the reaction occurs in the gas phase or at the particle surface. The isomeric n-alkanones have a higher reaction formation probability from the 3-position to middle position of the carbon chain in the homogeneous reaction pathways, and a slightly lower abundance at the 2-position, whereas the H-abstraction occurs preferentially at the 2-position of the carbon chain in the heterogeneous reaction pathways (Zhang et al., 2015; Ruehl et al., 2013). Thus, n-alkan-2-one/n-alkan-3-one ratios with the same carbon number are higher than one in the heterogeneous reaction pathways, while in the homogeneous reaction pathways they are lower than one. The ratios of n-alkan-2-one/n-alkan-3-one (C_8-C_{30}) with the same carbon atom number were calculated (Fig. 7b), with an average of 2.89 (0.69–8.07) at the IAP in Beijing, with an average 4.55 (1.55–8.63) at RU in London. The difference between IAP and RU probably reflects different predominant primary emission sources in the two cities, but there are many similarities in the C_8-C_{18} range (Fig. 7b).

3.4. Furanones (γ-lactones) and 6, 10, 14-trimethylpentadecan-2-one

A number of the (n-C_0-n-C_{14})-dihydro-2(3H)-furanones have been previously identified in the organic aerosol (Alves et al., 2001; Greaves et al., 1987; Hamilton et al., 2004), and were believed to arise from the photo-oxidized products of n-alkanals (Forstner et al., 1997). Another precursor of dihydro-2(3H)-furanones is n-alkenes, and n-C_2, n-C_3, and n-C_5-dihydro-2(3H)-furanones have been identified from a chamber study during the photo-oxidation of 1-decene (Forstner et al., 1997). The n-C_4 to n-C_{14}-dihydro-2(3H)-furanones were identified in the Beijing samples, and concentrations ranged from 0.43 to 3.99 ng m^{-3} (Table S2). The average Σ furanones was 20.5 ± 24.4 ng m^{-3} during haze episodes, increased more than twofold compared to the non-haze period (8.52 ± 4.46 ng m^{-3}).

Furanones are emitted from food cooking, and published profiles of compounds reviewed by Abdullahi et al. (2013) show a wide

distribution from 5-ethyldihydro-2(3H)-furanone to 5-tetra-decyldihydro-2(3H)-furanone, with a peak in abundance at the C_{11} and C_{12} – dihydro-2(3H)-furanones. This bears similarity to our data for this compound group shown in Table S2 and it seems likely, especially given the relatively low atmospheric concentrations that food cooking is a substantial contributor.

In all samples, one of the predominant ketones found in the atmospheric aerosol was phytone (6, 10, 14-trimethylpentadecan-2-one) which is a degradation product of phytol and has been proposed as a marker for secondary biogenic aerosol (Andreou and Rapsomanikis, 2009; Oliveira et al., 2007), even though it was identified in coal smoke particulate matter (Oros and Simoneit, 2000) with a really low emission rate. The ketone has been reported as an abundant compound in rural samples from a forest area (Oliveira et al., 2007), with concentrations of approximately 289–459 ng m^{-3}. In Beijing, the average concentration of phytone was 14.7 $\pm$ 11.7 ng m^{-3}.

4. Conclusions

Seven classes of compounds, including n-alkanes, n-alkenes, n-alkanals, n-alkan-2-ones, n-alkan-3-ones, furanones and phytone, were determined in the fine particle samples from Beijing. The PM$_{2.5}$, OC and BC were simultaneously determined. More than one hundred organic compounds were identified in this study, and the total concentrations of identified organic compounds were 744 $\pm$ 510 ng m^{-3}, accounting for 0.36–5.91% (average 2.47%) of OM. Higher average concentrations were measured for n-alkanes (C_{10}-C_{36}) and n-alkenes (C_{12}-C_{26}) in PM$_{2.5}$ in Beijing,. Several diagnostic criteria were used to qualitatively reconcile the sources of n-alkanes, and the results demonstrated that fossil fuel combustion represented the main source of identifiable n-alkanes and n-alkenes. Aliphatic carbonyls, including n-alkanals (C_8-C_{29}), n-alkan-2-ones (C_8-C_{31}) and n-alkan-3-ones (C_8-C_{30}), were measured in samples, and coal combustion appeared to be the dominant source of the high molecular weight carbonyl compounds. For the carbonyl compounds with low carbon numbers, the n-alkanals were linked to vehicle emissions, whereas the OH oxidation of n-alkanes was considered as a contributor to n-alkan-2-ones and n-alkan-3-ones. The average homologue profiles in Beijing and London show appreciable differences for all compound groups, suggesting different predominant sources. In London, diesel emissions are a major source with roadside concentrations (at MR) far exceeding those at Regent's University for all compound groups, but especially for n-alkanes. In Beijing, there appears to be a substantial contribution of other sources, with coal combustion being an obvious contributor. A substantial contribution of cooking emissions to the majority of compounds measured in this study seems unlikely.

The low M.W. furanones (γ-lactones) could be mechanistically linked as SOA products of gas phase hydrocarbon precursor oxidation with a large number being attributable to aliphatic aldehyde oxidation. However, especially for the higher M.W. compounds, food cooking is a probable source. One of the predominant ketones found in the atmospheric aerosol samples was phytone (6, 10, 14-trimethylpentadecan-2-one), usually considered as the photooxidation products of phytol, indicating a biogenic emission input.

Acknowledgements

Appendix A. Supplementary data

Supplementary data to this article can be found online at https://doi.org/10.1016/j.atmosenv.2019.01.023.

References

Abdullahi, K.L., Delgado-Saborit, J.M., Harrison, R.M., 2013. Emissions and indoor concentrations of particulate matter and its specific chemical components from cooking: a review. Atmos. Environ. 71, 260–294.

Alam, M.S., Harrison, R.M., 2016. Recent advances in the application of 2-dimensional gas chromatography with soft and hard ionisation time-of-flight mass spectrometry in environmental analysis. Chem. Sci. 7, 3968–3977.

Alam, M.S., Zeraati-Rezaei, S., Stark, C.P., Liang, Z., Xu, H., Harrison, R.M., 2016a. The characterisation of diesel exhaust particles - composition, size distribution and partitioning. Faraday Discuss 189, 69–84.

Alam, M.S., Stark, C., Harrison, R.M., 2016b. Using variable ionization energy time-of-flight mass spectrometry with comprehensive GC × GC to identify isomeric species. Anal. Chem. 88, 4211–4220.

Alam, M.S., Zeraati-Rezaei, S., Liang, Z., Stark, C., Xu, H., MacKenzie, A.R., Harrison, R.M., 2018. Mapping and quantifying isomer sets of hydrocarbons (≥ C 12) in diesel exhaust, lubricating oil and diesel fuel samples using GC× GC-ToF-MS. Atmos. Meas. Tech. 11, 3047–3058.

Alves, C., Pio, C., Duarte, A., 2001. Composition of extractable organic matter of air particles from rural and urban Portuguese areas. Atmos. Environ. 35, 5485–5496.

Andreou, G., Rapsomanikis, S., 2009. Origins of n-alkanes, carbonyl compounds and molecular biomarkers in atmospheric fine and coarse particles of Athens, Greece. Sci. Total Environ. 407, 5750–5760.

Bi, X., Sheng, G., Peng, P. a., Chen, Y., Zhang, Z., Fu, J., 2003. Distribution of particulate- and vapor-phase n-alkanes and polycyclic aromatic hydrocarbons in urban atmosphere of Guangzhou, China. Atmos. Environ. 37, 289–298.

Bray, E., Evans, E., 1961. Distribution of n-paraffins as a clue to recognition of source beds. Geochim. Cosmochim. Acta 22, 2–15.

Cao, J.-J., Zhu, C.-S., Tie, X.-X., Geng, F.-H., Xu, H.-M., Ho, S., Wang, G.-H., Han, Y.-M., Ho, K.-F., 2013. Characteristics and sources of carbonaceous aerosols from Shanghai, China. Atmos. Chem. Phys. 13, 803–817.

Cheng, Y., Li, S.-M., Leithead, A., Brook, J.R., 2006. Spatial and diurnal distributions of n-alkanes and n-alkan-2-ones on PM$_{2.5}$ aerosols in the Lower Fraser Valley, Canada. Atoms. Environ. 40, 2706–2720.

Cheng, Y., Engling, G., He, K.-B., Duan, F.-K., Ma, Y.-L., Du, Z.-Y., Liu, J.-M., Zheng, M., Weber, R.J., 2013. Biomass burning contribution to Beijing aerosol. Atmos. Chem. Phys. 13, 7765–7781.

Chrysikou, L.P., Samara, C.A., 2009. Seasonal variation of the size distribution of urban particulate matter and associated organic pollutants in the ambient air. Atmos. Environ. 43, 4557–4569.

Duan, J., Tan, J., Yang, L., Wu, S., Hao, J., 2008. Concentration, sources and ozone formation potential of volatile organic compounds (VOCs) during ozone episode in Beijing. Atmos. Res. 88, 25–35.

Fan, X., Lang, J., Cheng, S., Wang, X., Lü, Z., 2018. Seasonal variation and source analysis for PM$_{2.5}$, PM$_1$ and their carbonaceous components in Beijing. Huan Jing Ke Xue 39, 4430–4438. https://doi.org/10.13227/j.hjkx.201801186.

Feng, J., Hu, M., Chan, C.K., Lau, P.S., Fang, M., He, L., Tang, X., 2006. A comparative study of the organic matter in PM$_{2.5}$ from three Chinese megacities in three different climatic zones. Atmos. Environ. 40, 3983–3994.

Forstner, H.J., Flagan, R.C., Seinfeld, J.H., 1997. Molecular speciation of secondary organic aerosol from photooxidation of the higher alkenes: 1-octene and 1-decene. Atmos. Environ. 31, 1953–1964.

Gogou, A., Stratigakis, N., Kanakidou, M., Stephanou, E.G., 1996. Organic aerosols in Eastern Mediterranean: components source reconciliation by using molecular markers and atmospheric back trajectories. Org. Geochem. 25, 79–96.

Greaves, R.C., Barkley, R.M., Sievers, R.E., Meglen, R.R., 1987. Covariations in the concentrations of organic compounds associated with springtime atmospheric aerosols. Atmos. Environ. 21, 2549–2561.

Hamilton, J., Webb, P., Lewis, A., Hopkins, J., Smith, S., Davy, P., 2004. Partially oxidised organic components in urban aerosol using GCxGC-TOF/MS. Atmos. Chem. Phys. 4, 1279–1290.

Han, D., Fu, Q., Gao, S., Xu, H., Liang, S., Cheng, P., Chen, X., Zhou, Y., Cheng, J., 2018. Non-polar organic compounds in aerosols in a typical city of Eastern China: size distribution, gas-particle partitioning and tracer for PM$_{2.5}$ source apportionment. Atmos. Chem. Phys. 18, 9375–9391.

He, L.-Y., Hu, M., Huang, X.-F., Zhang, Y.-H., Tang, X.-Y., 2006. Seasonal pollution characteristics of organic compounds in atmospheric fine particles in Beijing. Sci. Total Environ. 359, 167–176.

Hong, Z., Hong, Y., Zhang, H., Chen, J., Xu, L., Deng, J., Du, W., Zhang, Y., Xiao, H., 2017. Pollution characteristics and source apportionment of PM$_{2.5}$-bound n-alkanes in the yangtze river delta, China. Aerosol Air Qual. Res. 17, 1985–1998.

Huang, R.-J., Zhang, Y., Bozzetti, C., Ho, K.-F., Cao, J.-J., Han, Y., Daellenbach, K.R., Slowik, J.G., Platt, S.M., Canonaco, F., 2014. High secondary aerosol contribution to particulate pollution during haze events in China. Nature 514. https://doi.org/10.1038/nature13774.

Kang, M., Ren, L., Ren, H., Zhao, Y., Kawamura, K., Zhang, H., Wei, L., Sun, Y., Wang, Z., Fu, P., 2018. Primary biogenic and anthropogenic sources of organic aerosols in Beijing, China: insights from saccharides and n-alkanes. Environ. Pollut. 243, 1579–1587.

Kwok, E.S., Atkinson, R., 1995. Estimation of hydroxyl radical reaction rate constants for gas-phase organic compounds using a structure-reactivity relationship: an update. Atmos. Environ. 29, 1685–1695.

Lang, J., Zhang, Y., Zhou, Y., Cheng, S., Chen, D., Guo, X., Chen, S., Li, X., Xing, X., Wang, H., 2017. Trends of PM$_{2.5}$ and chemical composition in Beijing, 2000–2015. Aerosol Air Qual. Res. 17, 412–425.

Li, W., Peng, Y., Bai, Z., 2010. Distributions and sources of n-alkanes in PM2.5 at urban, industrial and coastal sites in Tianjin, China. J. Environ. Sci. 22, 1551–1557.

Li, Y., Cao, J., Li, J., Zhou, J., Xu, H., Zhang, R., Ouyang, Z., 2013. Molecular distribution and seasonal variation of hydrocarbons in PM2.5 from Beijing during 2006. Particuology 11, 78–85.

Liu, Y., Yan, C., Zheng, M., 2018. Source apportionment of black carbon during winter in Beijing. Sci. Total Environ. 618, 531–541.

Lyu, Y., Xu, T., Yang, X., Chen, J., Cheng, T., Li, X., 2017. Seasonal contributions to size-resolved n-alkanes (C8–C40) in the Shanghai atmosphere from regional anthropogenic activities and terrestrial plant waxes. Sci. Total Environ. 579, 1918–1928.

Lyu, R., Shi, Z., Alam, M.S., Wu, X., Liu, D., Vu, T.V., Stark, C., Fu, P., Feng, Y., Harrison, R.M., 2018. Alkanes and aliphatic carbonyl compounds in wintertime PM2.5 in Beijing, China. Atmos. Chem. Phys submitted.

Matsunaga, A., Docherty, K.S., Lim, Y.B., Ziemann, P.J., 2009. Composition and yields of secondary organic aerosol formed from OH radical-initiated reactions of linear alkenes in the presence of NOx: modeling and measurements. Atmos. Environ. 43, 1349–1357.

Oliveira, T.S., Pio, C., Alves, C.A., Silvestre, A.J., Evtyugina, M., Afonso, J., Fialho, P., Legrand, M., Puxbaum, H., Gelencsér, A., 2007. Seasonal variation of particulate lipophilic organic compounds at nonurban sites in Europe. J. Geophys. Res.: Atmosphere 112, D23S09. https://doi.org/10.1029/2007JD008504.

Oros, D.R., Simoneit, B.R.T., 2000. Identification and emission rates of molecular tracers in coal smoke particulate matter. Fuel 79, 515–536.

Presto, A.A., Miracolo, M.A., Donahue, N.M., Robinson, A.L., 2010. Secondary organic aerosol formation from high-NOx photo-oxidation of low volatility precursors: n-Alkanes. Environ. Sci. Technol. 44, 2029–2034.

Ren, L., Fu, P., He, Y., Hou, J., Chen, J., Pavuluri, C.M., Sun, Y., Wang, Z., 2016. Molecular distributions and compound-specific stable carbon isotopic compositions of lipids in wintertime aerosols from Beijing. Sci. Rep. 6, 27481. https://doi.org/10.1038/srep27481.

Rogge, W.F., Hildemann, L.M., Mazurek, M.A., Cass, G.R., Simoneit, B.R.T., 1993. Sources of fine organic aerosol. 4. Particulate abrasion products from leaf surfaces of urban plants. Environ. Sci. Technol. 27, 2700–2711.

Rogge, W.F., Hildemann, L.M., Mazurek, M.A., Cass, G.R., 1998. Sources of fine organic aerosol. 9. Pine, oak, and synthetic log combustion in residential fireplaces. Environ. Sci. Technol. 32, 13–22.

Ruehl, C.R., Nah, T., Isaacman, G., Worton, D.R., Chan, A.W.H., Kolesar, K.R., Cappa, C.D., Goldstein, A.H., Wilson, K.R., 2013. The Influence of molecular structure and aerosol phase on the heterogeneous oxidation of normal and branched alkanes by OH. J. Phys. Chem. A 117, 3990–4000.

Schauer, J.J., Kleeman, M.J., Cass, G.R., Simoneit, B.R.T., 1999a. Measurement of emissions from air pollution sources. 1. C1 through C29 organic compounds from meat charbroiling. Environ. Sci. Technol. 33, 1566–1577.

Schauer, J.J., Kleeman, M.J., Cass, G.R., Simoneit, B.R.T., 1999b. Measurement of emissions from air pollution sources. 2. C1 through C30 organic compounds from medium duty diesel trucks. Environ. Sci. Technol. 33, 1578–1587.

Schauer, J.J., Kleeman, M.J., Cass, G.R., Simoneit, B.R.T., 2002. Measurement of emissions from air pollution sources. 5. C1−C32 organic compounds from gasoline-powered motor vehicles. Environ. Sci. Technol. 36, 1169–1180.

Schilling Fahnestock, K.A., Yee, L.D., Loza, C.L., Coggon, M.M., Schwantes, R., Zhang, X., Dalleska, N.F., Seinfeld, J.H., 2015. Secondary organic aerosol composition from C12 alkanes. J. Phys. Chem. A 119, 4281–4297.

Seinfeld, J.H., Pandis, S.N., 2016. Atmospheric Chemistry and Physics: from Air Pollution to Climate Change, third ed. John Wiley & Sons, Inc, Hoboken, NJ.

Shi, Z., Vu, T., Kotthaus, S., Fu, P., Zhu, T., Han, Y., Lee, J., Demuzere, M., Grimmond, S., Dunmore, R., Yue, S., Ren, L., He, K., Zhang, Q., Lewis, A., Kelly, F., Loh, M., Sun, Z., Guan, D., Tao, S., Jones, R., Popoola, O., Bloss, W., Liu, D., Wang, X., Zhang, L., Li, J., Sun, Y., Shao, L., Wang, W., Tong, S., Wu, Z., Xie, P., Li, W., Heard, D., Whalley, L., Hewitt, N., Wild, O., Allan, J., Coe, H., Nemitz, E., Hamilton, J., Yang, F., Ji, D., Harrison, R.M., 2018. Introduction to Special Issue: in-depth study of air pollution sources and processes within Beijing and its surrounding region (APHH-Beijing). Atmos. Chem. Phys. Discuss. https://doi.org/10.5194/acp-2018-922.

Simoneit, B.R., 1985. Application of molecular marker analysis to vehicular exhaust for source reconciliations. Int. J. Environ. Anal. Chem. 22, 203–232.

Simoneit, B.R.T., 1989. Organic matter of the troposphere - V: application of molecular marker analysis to biogenic emissions into the troposphere for source reconciliations. J. Atmos. Chem. 8, 251–275.

Simoneit, B., Rogge, W., Lang, Q., Jaffé, R., 2000. Molecular characterization of smoke from campfire burning of pine wood (Pinus elliottii). Chemosphere Global Change Sci. 2, 107–122.

Simoneit, B.R.T., 2002. Biomass burning – a review of organic tracers for smoke from incomplete combustion. Appl. Geochem. 17, 129–162.

Simoneit, B.R.T., Kobayashi, M., Mochida, M., Kawamura, K., Lee, M., Lim, H.-J., Turpin, B.J., Komazaki, Y., 2004. Composition and major sources of organic compounds of aerosol particulate matter sampled during the ACE-Asia campaign. J. Geophys. Res.: Atmosphere 109, D19S10. https://doi.org/10.1029/2004JD004598.

Turpin, B.J., Lim, H.-J., 2001. Species contributions to PM2.5 mass concentrations: revisiting common assumptions for estimating organic mass. Aerosol Sci. Technol. 35, 602–610.

Wang, G., Kawamura, K., 2005. Molecular characteristics of urban organic aerosols from Nanjing: a case study of a mega-city in China. Environ. Sci. Technol. 39, 7430–7438.

Wang, G., Kawamura, K., Lee, S., Ho, K., Cao, J., 2006. Molecular, seasonal, and spatial distributions of organic aerosols from fourteen Chinese cities. Environ. Sci. Technol. 40, 4619–4625.

Wang, Q., Feng, Y., Huang, X., Griffith, S.M., Zhang, T., Zhang, Q., Wu, D., Yu, J.Z., 2016. Nonpolar organic compounds as PM2.5 source tracers: investigation of their sources and degradation in the Pearl River Delta, China. J. Geophys. Res. Atmos. 121 (11). https://doi.org/10.1002/2016JD025315. 862-11,879.

Wu, X., Vu, T.V., Shi, Z., Harrison, R.M., Liu, D., Cen, K., 2018. Characterization and source apportionment of carbonaceous PM2.5 particles in China - a review. Atmos. Environ. 189, 187–212.

Wu, W., Zhao, B., Wang, S., Hao, J., 2017. Ozone and secondary organic aerosol formation potential from anthropogenic volatile organic compounds emissions in China. J. Environ. Sci. 53, 224–237.

Xu, H., Tao, J., Ho, S.S.H., Ho, K., Cao, J., Li, N., Chow, J.C., Wang, G., Han, Y., Zhang, R., 2013. Characteristics of fine particulate non-polar organic compounds in Guangzhou during the 16th Asian Games: effectiveness of air pollution controls. Atmos. Environ. 76, 94–101.

Xu, X., Zhang, H., Chen, J., Li, Q., Wang, X., Wang, W., Zhang, Q., Xue, L., Ding, A., Mellouki, A., 2018. Six sources mainly contributing to the haze episodes and health risk assessment of PM2.5 at Beijing suburb in winter 2016. Ecotoxicol. Environ. Saf. 166, 146–156.

Yadav, S., Tandon, A., Attri, A.K., 2013. Characterization of aerosol associated non-polar organic compounds using TD-GC-MS: a four year study from Delhi, India. J. Hazard Mater. 252, 29–44.

Yan, C., Zheng, M., Sullivan, A.P., Bosch, C., Desyaterik, Y., Andersson, A., Li, X., Guo, X., Zhou, T., Gustafsson, Ö., Collett, J.L., 2015. Chemical characteristics and light-absorbing property of water-soluble organic carbon in Beijing: biomass burning contributions. Atmos. Environ. 121, 4–12.

Yang, X., Cheng, S., Wang, G., Xu, R., Wang, X., Zhang, H., Chen, G., 2018. Characterization of volatile organic compounds and the impacts on the regional ozone at an international airport. Environ. Pollut. 238, 491–499.

Yao, L., Yang, L., Yuan, Q., Yan, C., Dong, C., Meng, C., Sui, X., Yang, F., Lu, Y., Wang, W., 2016. Sources apportionment of PM2.5 in a background site in the North China Plain. Sci.Tot. Environ. 541, 590–598.

Zhang, H., Worton, D.R., Shen, S., Nah, T., Isaacman-VanWertz, G., Wilson, K.R., Goldstein, A.H., 2015. Fundamental time scales governing organic aerosol multiphase partitioning and oxidative aging. Environ. Sci. Technol. 49, 9768–9777.

Zhang, T., Claeys, M., Cachier, H., Dong, S., Wang, W., Maenhaut, W., Liu, X., 2008. Identification and estimation of the biomass burning contribution to Beijing aerosol using levoglucosan as a molecular marker. Atmos. Environ. 42, 7013–7021.

Zhao, Y., Hu, M., Slanina, S., Zhang, Y., 2007. Chemical compositions of fine particulate organic matter emitted from Chinese cooking. Environ. Sci. Technol. 41, 99–105.

Zhu, C., Tian, H., Cheng, K., Liu, K., Wang, K., Hua, S., Gao, J., Zhou, J., 2016. Potentials of whole process control of heavy metals emissions from coal-fired power plants in China. J. Clean. Prod. 114, 343–351.